

Interstitial carbon-oxygen center and hydrogen related shallow thermal donors in Si

J. Coutinho and R. Jones

School of Physics, University of Exeter, Exeter EX4 4QL, United Kingdom

P. R. Briddon

Department of Physics, University of Newcastle upon Tyne, Newcastle upon Tyne NE1 7RU, United Kingdom

S. Öberg

Department of Mathematics, Luleå University of Technology, Luleå S-97187, Sweden

L. I. Murin

Institute of Solid State and Semiconductor Physics, Minsk 220072, Belarus

V. P. Markevich

Department of Electrical Engineering and Electronics and Centre for Electronic Materials, University of Manchester Institute of Science and Technology, Sackville Street, Manchester M601QD, United Kingdom

J. L. Lindström

Department of Physics, University of Lund, S-221 00 Lund, Sweden

(Received 23 July 2001; published 10 December 2001)

The interstitial carbon-oxygen defect is a prominent defect formed in e -irradiated Cz-Si containing carbon. Previous stress alignment investigations have shown that the oxygen atom weakly perturb the carbon interstitial but the lack of a high-frequency oxygen mode has been taken to imply that the oxygen atom is severely affected and becomes overcoordinated. Local vibrational mode spectroscopy and *ab initio* modeling are used to investigate the defect. We find new modes whose oxygen isotopic shifts give further evidence for oxygen overcoordination. Moreover, we find that the calculated stress-energy tensor and energy levels are in good agreement with experimental values. The complexes formed by adding both single (C_iO_iH) and a pair of H atoms ($C_iO_iH_2$), as well as the addition of a second oxygen atom, are considered theoretically. It is shown that the first is bistable with a shallow donor and deep acceptor level, while the second is passive. The properties of C_iO_iH and C_iO_2H are strikingly similar to the first two members of a family of shallow thermal donors that contain hydrogen.

DOI: 10.1103/PhysRevB.65.014109

PACS number(s): 61.72.Bb, 61.72.Ji, 61.80.Az, 63.20.Pw

I. INTRODUCTION

Low-temperature e -irradiation of Si generates mobile Si interstitials which are readily trapped by substitutional carbon defects forming carbon interstitials (C_i).¹ In turn, these are mobile at room temperature and subsequently complex with many impurities including oxygen. The interstitial carbon-oxygen center (C_iO_i) is a product of the latter interaction and is a stable defect with an annealing temperature around 350–450 °C. It has been detected by all four principal methods used to characterize defects. Electron paramagnetic resonance (EPR) experiments relate the G15 signal to $C_iO_i^{(+)}$. The similarity of its magnetic properties with that of the carbon interstitial implies that the C atom is only slightly affected by oxygen which is assumed to be bonded to remote Si atoms such as Si_2 and Si_3 shown in Fig. 1(a).^{2,3}

The defect gives a prominent 0.7896 eV photoluminescent (PL) signal (C band),⁴ associated with several local mode replicas.^{5,6} Previous Fourier transform infrared (FTIR) spectroscopic experiments have identified local vibrational modes (LVM's) at 1116, 865, 742, 550, and 529.8 cm^{-1} , the highest of which is carbon and not oxygen related.⁷ Finally, deep-level transient spectroscopy (DLTS) has linked a donor

level at $E_v + 0.38$ eV with the defect.⁸

Earlier theoretical modeling had found that the oxygen atom was strongly affected by carbon and was not divalent as in Fig. 1(a), but rather was bonded to three Si atoms as illustrated in Fig. 1(b).^{9,10} This is because the greater electronegativity of carbon encouraged electron transfer from the Si_2 atom with the dangling bond shown in Fig. 1(a). This leaves the dangling bond orbital empty and leads to a dative bond with a lone pair orbital on oxygen. Thus the oxygen

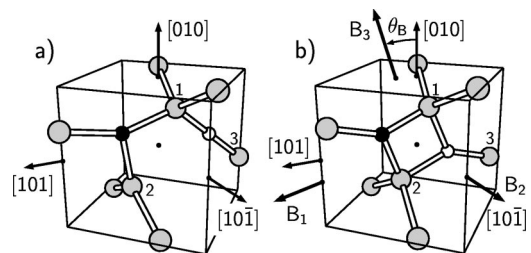


FIG. 1. Models for C_iO_i . (a) Divalent oxygen model, (b) trivalent oxygen model. Gray, black, white atoms are Si, C, O. Crystallographic axes and principal directions of the B tensor are also shown.

atom is trivalent. Overcoordinated oxygen atoms are currently of interest because of their possible role in thermal donor defects.¹¹

The main evidence in support of this model lay in the lack of any mode around 1136 cm^{-1} related to bond-centered interstitial oxygen (O_i). However, not all the local modes of the defect had been found and especially their oxygen isotopic shifts. In this paper we present further vibrational mode evidence supporting the model and demonstrate that its calculated donor level and stress-energy, or piezospectroscopic, tensor are in agreement with the observations.

Further interest in the defect has recently arisen from the observation of a marked reduction in its concentration in irradiated samples into which hydrogen had been introduced by wet etching.¹² These studies suggested that the C_iO_i defect can trap up to two hydrogen atoms and that the single hydrogenated center possessed a deep hole trap H4 at $E_v + 0.28\text{ eV}$. However, recent work has reassigned H4 to the (+/0) level of the vacancy-oxygen-hydrogen (VOH) complex.¹³

In view of these developments, we have investigated the interaction of the defect with hydrogen, paying attention to its electrical properties. It is clear that the defect with two H atoms is inert but a single H atom results in a bistable defect with intriguing properties. In one form, it behaves as a deep acceptor, but in another configuration, it is a shallow donor. The calculated configuration energy curves for the defect are strikingly similar to a hydrogen related radiation-induced shallow donor labeled D1. Moreover, the calculated oxygen related vibrational mode and its anomalous upward shift with hydrogen are close to the values observed for D1.

This defect appears to be the first of a family of shallow single donors which are successively produced on annealing e -irradiated Czochralski-grown Si (Cz-Si) into which hydrogen had been introduced.¹⁴ The first two members D1 and D2 are formed around $350\text{ }^\circ\text{C}$ and $450\text{ }^\circ\text{C}$, respectively, and have (0/+) levels at $E_c - 42.6\text{ meV}$ and $E_c - 37.0\text{ meV}$ which are comparable with phosphorus ($E_c - 45.6\text{ meV}$). The defects possess a Rydberg series of excited states, and the effective-mass IR transitions for D2 and D3 are identical with those of the shallow thermal donors STD(H)2 and STD(H)3 found by annealing O-rich Si containing hydrogen.^{15,16} The STD(H) N family members are known to contain hydrogen as their electronic transitions shift in deuterated material. However, the STD defects are formed in annealed Cz-Si without prior irradiation and they have been suggested to be responsible for the NL10(H) family of shallow single thermal donors.¹⁵ It has also been proposed that these centers contain, in addition to hydrogen, interstitial carbon and oxygen.^{17,18} However, there is no spectroscopic evidence for these impurities in the DN and STD(H) N families. Nevertheless, weak ^{17}O -hyperfine satellites have been found in NL10 shallow donors in Al-doped samples.^{19,20}

A considerable body of information about D1 has been found by electrical, photoelectrical, optical, and magnetic experiments.^{14,21–25} Thus it is known that the defect is bistable, assuming the H form in the positive and neutral-charge states and the D form in the negative-charge state. A metastable neutral D form (originally labeled X) also exists. Hall effect and conductivity studies show that the defect has

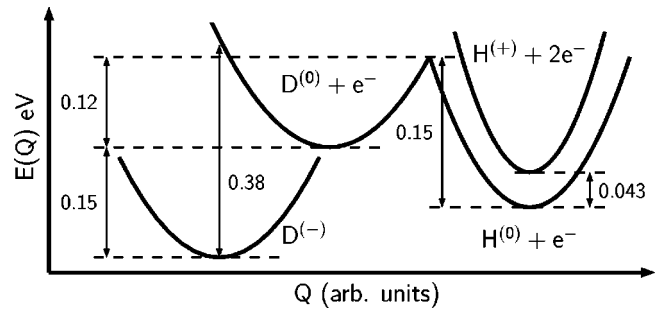


FIG. 2. Configuration coordinate diagram for D1 according to Markevich *et al.* (Ref. 23). Quoted energies are based on electrical, optical, and capacitance measurements.

a negative U with an occupation level (the average of the donor and acceptor levels) at $E_c - 0.076\text{ eV}$. Electronic IR absorption studies show a donor level lying 43 meV below the conduction band and this then places the acceptor level, or the difference between $\text{D}^{(-)}$ and $\text{H}^{(0)}$, at $E_c - 0.11\text{ eV}$. DLTS and optical absorption studies were used to determine the other energies in the configuration coordinate diagram shown in Fig. 2.

The D form of D1 has also been correlated with a local vibrational mode at 1025.5 cm^{-1} that shifts *upwards* to 1027.9 cm^{-1} with deuterium, demonstrating that this defect contains H.²⁵ This unusual shift has not been explained previously but here we link it to an anticrossing with an unobserved carbon-hydrogen wag mode. No vibrational modes have been found for the H form.

The neutral H form of D1 has also been associated with an EPR center labeled TU1 detected under illumination conditions.²⁴ Its isotropic g tensor probably arises from the delocalized spin density which does not reflect the true symmetry of the defect. One ^{29}Si -hyperfine satellite has been resolved having an isotropic interaction of about 60 MHz . Comparing this with the isotropic hyperfine interaction of 4594 MHz arising from a free ^{29}Si atom²⁶ gives 1.3% of the spin density located on this unique atom. Hyperfine interactions with hydrogen were recently observed for D1 and D2 by using electron-nuclear double-resonance (ENDOR) spectroscopy.²⁷ One principal axis of the hyperfine tensor is nearly parallel to the $\langle 110 \rangle$ direction, suggesting a H bond lying along this direction. The isotropic part of the hyperfine tensor corresponds to a minute spin density on H of $6 \times 10^{-3}\%$. Similar densities and hyperfine tensors were measured for the NL10(H) defects,²⁸ strengthening the link between the STD(H) N , NL10(H), and DN families.

It has been suggested that D1 is a complex of hydrogen with an oxygen-related radiation-induced defect like VO or C_iO_i .¹⁴ However, VOH is an acceptor with a level at $E_c - 0.31\text{ eV}$,^{29–32} while VOH_2 is passive.³³ In this paper, we show that D1 has many properties in common with $\text{C}_i\text{O}_i\text{H}$. This in turn suggests that the shallow thermal donors STD(H) N also contain interstitial carbon. It is known that interstitial carbon can be produced as a by-product of oxygen aggregation in annealed Cz-Si and does not require irradiation for its formation. This follows as annealing Cz-Si to about $450\text{ }^\circ\text{C}$ produces a set of prominent photoluminescent

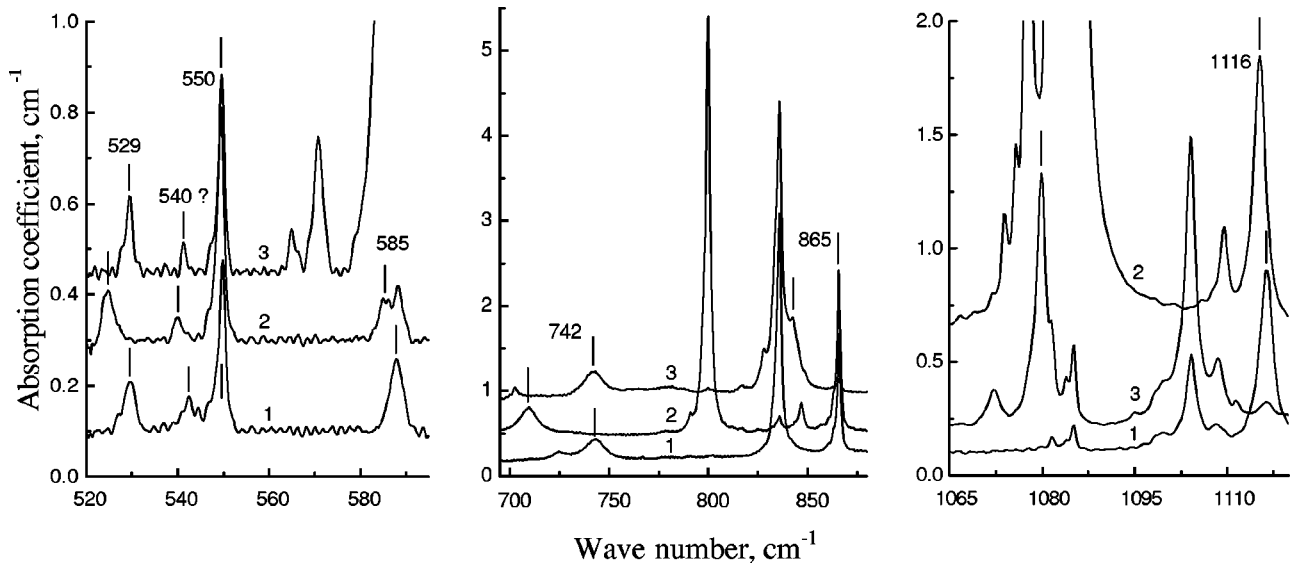


FIG. 3. Sections of the absorption spectra measured at 10 K for electron-irradiated Si samples: (1) $[^{16}\text{O}] = 1 \times 10^{18}$ and $[^{12}\text{C}] = 3 \times 10^{17}$ cm^{-3} , irradiation dose $F = 1 \times 10^{18}$ cm^{-2} ; (2) $[^{18}\text{O}] = 1.5 \times 10^{18}$, $[^{16}\text{O}] = 5 \times 10^{16}$, and $[^{12}\text{C}] = 4 \times 10^{17}$ cm^{-3} , $F = 1.5 \times 10^{18}$ cm^{-2} ; (3) $[^{16}\text{O}] = 1 \times 10^{18}$, $[^{13}\text{C}] = 1.5 \times 10^{18}$, and $[^{12}\text{C}] = 2 \times 10^{17}$ cm^{-3} , $F = 1.5 \times 10^{18}$ cm^{-2} . The lines related to the C_iO_i complex are labeled.

lines. One of these is the T line at 0.935 eV which is known to be a complex involving interstitial carbon bonded to hydrogen and is stable up to ~ 600 $^\circ\text{C}$.³⁴ This thermal stability is comparable with the STD(H) N family which disappear around 550 $^\circ\text{C}$.¹⁶

The plan of this paper is as follows. Sections II and III deal with the experimental method and the measurements respectively. Sections IV and V describe the theoretical method and results for the C_iO_i , $\text{C}_i\text{O}_i\text{H}$, $\text{C}_i\text{O}_i\text{H}_2$, and $\text{C}_i\text{O}_2\text{H}$ defects. Finally, we give our conclusions in Sec. VI.

II. EXPERIMENTAL DETAILS

The IR absorption analysis was carried out using a Bruker 113v Fourier Transform IR Spectrometer. The measurements were performed at 10 K and at room temperature (RT), with a spectral resolution of 0.5–1.0 cm^{-1} . Three types of Si:O,C samples were used. The first (1) contained ^{16}O and ^{12}C , while the second (2) contained mainly ^{18}O and ^{12}C . The third (3) was doped with ^{16}O and ^{13}C . Samples (1) were fabricated from ordinary phosphorus-doped Cz-Si with initial resistivity of 60 Ω cm, with oxygen and carbon concentrations of about 1×10^{18} cm^{-3} and 3×10^{17} cm^{-3} , respectively. Samples (2) and (3) consisted of float-zone Si material (Fz-Si) enriched with oxygen and carbon isotopes. In (2) the concentrations of $^{16}\text{O}_i$, $^{18}\text{O}_i$, and $^{12}\text{C}_s$ were 5×10^{16} , 1.5×10^{18} , and 4×10^{17} cm^{-3} , respectively, while (3) contained about 1×10^{18} cm^{-3} of $^{16}\text{O}_i$ and 1.5×10^{18} cm^{-3} of $^{13}\text{C}_s$. The concentrations of oxygen and carbon were monitored by measuring the room-temperature intensities of the absorption bands at 1107 ($^{16}\text{O}_i$), 1058 ($^{18}\text{O}_i$), 605 ($^{12}\text{C}_s$), and 587 cm^{-1} ($^{13}\text{C}_s$), respectively.^{35,36} Irradiation with electrons (2.5 MeV) was performed at RT. Isochronal anneals of 30 min were carried out up to 600 $^\circ\text{C}$ in nitrogen ambient.

III. EXPERIMENTAL RESULTS

Figure 3 shows fragments of differential absorption spectra of electron-irradiated Si samples doped with different O and C isotope combinations. The signal from a low-carbon Fz-Si reference sample was subtracted from each spectrum. In all the samples, the dominant radiation-induced defects were the A center (bands at 835.8 and 799.9 cm^{-1} for ^{16}O - and ^{18}O -doped Si, respectively) and the C_iO_i complex. Traces of bands recently assigned to C_iC_s (Ref. 37) were also observed.

The peak positions of the lines related to C_iO_i complex were determined by using a Lorentzian fitting procedure. Table I gives these frequencies and their ^{13}C and ^{18}O isotopic shifts. In descending frequency, they will be labeled as the 1116, 865, 742, 585, 550, 540, and 529 cm^{-1} bands respectively. Other than the 585 and 540 cm^{-1} modes, the bands are the same as those given earlier.^{5–7,36,38} However, only carbon isotope effects (^{12}C , ^{13}C , and ^{14}C) had previously been studied by IR absorption, and shifts were only found for the 1116 and 865 cm^{-1} lines.^{38,7} In the present study, we were able to detect very small carbon isotopic shifts (≤ 0.5 cm^{-1}) for the 742, 550, and 529 cm^{-1} bands (see Table I).

The shifts with ^{18}O for all the IR absorption lines given above are reported here for the first time. The most important result is the observation of a significant 33.4 cm^{-1} oxygen isotopic shift *only* for the 742 cm^{-1} band, clearly indicating its oxygen character. This shift is in agreement with observations based on PL vibrational spectroscopy which only detects A_1 modes.^{5,6,36} The present work then clearly shows that the highest oxygen-related frequency lies at 742 cm^{-1} , compared with 1136 cm^{-1} for O_i , and possesses an ^{18}O shift considerably smaller than that of the asymmetric stretch mode in O_i (51.4 cm^{-1}),³⁹ where the O atom bridges neighboring Si atoms. The 742 cm^{-1} band is unusually broad:

TABLE I. Observed and calculated local vibrational modes (cm^{-1}), for $\text{C}_i\text{O}_i^{(0)}$. The first three columns report absolute frequencies, whereas columns 4 onwards give their downward isotopic shifts. Calculated LVM's for $\text{C}_i\text{O}_i^{(+)}$ are given in brackets.

Obs.	$^{16}\text{O}, ^{12}\text{C}$		$^{16}\text{O}, ^{13}\text{C}$			$^{18}\text{O}, ^{12}\text{C}$			$^{18}\text{O}, ^{13}\text{C}$	
		Calc.	Obs.	Calc.	(Obs.)	Obs.	Calc.	(Obs.)	Obs.	Calc.
1116.3	1137.6	(1087.9)	36.4	37.7	(35.8)	1.0	1.0	(1.2)	38.8	(37.2)
865.9	876.1	(827.2)	23.9	24.5	(22.9)	0.15	0.1	(0.2)	24.6	(23.3)
742.8	759.6	(747.6)	0.5	0.3	(0.8)	33.4	35.6	(35.2)	35.8	(35.5)
~588	593.4	(576.5)	—	0.1	(0.1)	~3	3.2	(5.5)	3.3	(5.5)
549.8	555.8	(548.0)	0.2	0.3	(0.3)	0.3	0.2	(0.2)	0.5	(0.5)
~542	544.7	(535.2)	~0.5	0.1	(0.2)	~1.5	0.5	(1.8)	0.5	(1.8)
529.6	544.2	(533.4)	0.1	0.0	(0.0)	5.2	5.4	(2.3)	5.5	(2.4)

~10 cm^{-1} full width at half maximum.

The low intensity and spectral location have probably prevented the detection of the 585 cm^{-1} band previously. In Si: $^{16}\text{O}, ^{12}\text{C}$ this band is masked by the X line at 588.5 cm^{-1} due to the C_sO_i pair, as well as the fundamental mode at 589.1 cm^{-1} of $^{13}\text{C}_s$ which occurs with a natural abundance of 1.1%. However, the slight shift of the 585 cm^{-1} band that occurs in ^{18}O -doped material is enough to distinguish it. It appears likely that the same LVM has been also observed in the local mode structure of the photoluminescence C line as the most intense $L2$ feature at 72.5 meV.^{5,6,36}

There are some hints that another weak band at ~540 cm^{-1} is associated with the C_iO_i complex and is labeled “540?” in Fig. 3. In Si: $^{16}\text{O}, ^{12}\text{C}$ this band is superimposed on bands at 540.4 and 543.3 cm^{-1} due to C_iC_s .³⁷ However, it undergoes a ~1.5 cm^{-1} shift in Si: $^{18}\text{O}, ^{12}\text{C}$ samples, suggesting an oxygen defect. Moreover, since its isochronal annealing behavior is essentially the same as that of the other C_iO_i -related lines, we tentatively identify it with this defect.

All the bands related to C_iO_i anneal out between 300–400 °C along with bands related to VO. Simultaneously, there is a strong increase in the intensities of lines related to C_sO_i . Evidently, the annealing behavior of two dominant defects, C_iO_i and VO, are closely related. Either vacancies, generated upon A-center dissociation, are trapped by C_iO_i or C_i atoms liberated from C_iO_i interact with VO. In both cases, C_sO_i is formed.

IV. THEORETICAL METHOD

The defects were analyzed using a density functional *ab initio* modeling program (AIMPRO), with localized Gaussian basis functions in a supercell geometry. Details of the method have been described earlier.⁴⁰ In the present investigation 64-Si-atom supercells were used and integration over the Brillouin zone was accomplished using a 2^3 set of Monkhorst-Pack \mathbf{k} points.⁴¹ The basis functions consisted of the same Gaussian s and p orbitals as described earlier in an extensive treatment of oxygen defects in Si and Ge.⁴⁰ Specifically the basis was Si (4, 1), O (6, 1), C (4, 1), and H (2, 1) where (N, M) refer to the number of independent s - or p -like Gaussian functions placed at the nuclei and bond centers, respectively. Convergence tests were carried out using a much larger basis involving $M=2$. The Fourier transform of

the charge density was accomplished using reciprocal lattice vectors with energies up to 150 a.u. Tests with larger cutoffs did not lead to significantly different results reported here.

Vibrational modes were found from the energy second derivatives between atoms within the core of the defect, which are directly obtained from the supercell calculations. For some modes near the Raman frequency, it is necessary to evaluate the derivatives connecting more remote atoms, but usually these were taken from a Musgrave-Pople potential evaluated previously.⁴² The dynamical matrix was then constructed and the vibrational frequencies found by diagonalization.

The Mulliken bond population of a gap state n approximately describes its localization on an atom i . If the wave function $\psi_{n,\mathbf{k}}(\mathbf{r})$ is expanded in a basis of Bloch functions $B_{i,\mathbf{k}}(\mathbf{r})$ composed of localized orbitals, i.e.,

$$\psi_{n,\mathbf{k}}(\mathbf{r}) = \sum_i c_{n,\mathbf{k},i} B_{i,\mathbf{k}}(\mathbf{r}),$$

then the population on atom i is given by

$$p_n(i) = \frac{1}{N} \sum_{j,\mathbf{k}} c_{n,\mathbf{k},i} S_{ij}^{\mathbf{k}} c_{n,\mathbf{k},j}^*,$$

where $S_{i,j}^{\mathbf{k}}$ is the overlap matrix between two basis functions and N the number of \mathbf{k} points in the zone. It is important to average over the Brillouin zone as the localization of a defect band varies with \mathbf{k} .

An important characteristic of an anisotropic defect is the stress-energy or piezospectroscopic tensor.⁴³ In the absence of any imposed stress, isolated point defects are equally distributed over all orientations related by the symmetry of the lattice. However, applying a compressive stress across, say, a particular face results in an increase in energy of those defects exerting a compressive stress on this face and a decrease in the energy of those which impose a tensile stress. The increase in energy is written $\Delta E = \text{Tr } B \cdot \epsilon$ where ϵ is the imposed strain tensor and B is the energy-stress tensor. Since only the relative energies of defects with different orientations can be measured, only the traceless part of B is known.

To evaluate the B tensor, the volume of the supercell was first relaxed.⁴⁴ This ensures that the tensor is traceless and reduced the formation energy of C_iO_i by only 40 meV, sug-

TABLE II. Formation energies E_f , $E(-/0)$, $E(0/+)$, and acceptor $(-/0)$ and donor $(0/+)$ levels of O_i , C_i , C_iO_i , C_iO_iH , and $C_iO_{2i}H$ defects (eV). C_iO_iH and $C_iO_{2i}H$ defects have forms R and O. Values are calculated using Gaussian s,p orbitals with one set of Gaussian functions at bond-center sites (four orbitals), and bracketed values are runs with two Gaussians (eight orbitals). E_f was calculated by taking chemical potentials of Si, O, C, and H from silicon, α -quartz, diamond, and molecular H_2 environments, respectively. The last two columns are estimates of acceptor and donor levels relative to the band edges found as described in the text.

	E_f		$E(-/0)$		$E(0/+)$		$E_c(-/0)$		$(0/+)-E_v$	
O_i	1.809	(1.817)								
C_i	4.122	(4.056)	7.073	(6.963)	6.666	(6.603)				
C_iO_i	4.212	(4.107)			6.750	(6.731)			0.364	(0.408)
C_iO_iH (R)	3.309	(3.281)			7.506	(7.416)			1.120	(1.093)
C_iO_iH (O)	3.475	(3.331)	6.908	(6.865)			0.265	(0.198)		
$C_iO_{2i}H$ (R)	3.923	(3.858)			7.547	(7.419)			1.161	(1.096)
$C_iO_{2i}H$ (O)	4.479	(4.308)	6.859	(6.798)			0.314	(0.265)		

gesting that the cell is sufficiently large to treat the isolated center. The B tensor of a C_{1h} defect has one principal axis lying perpendicular to the mirror plane which we take to be $(10\bar{1})$. The tensor has then three independent elements corresponding to two independent principal values and one angle.

Four different strain tensors e_{xx} , e_{yy} , e_{xy} , and e_{xz} were applied to the unit-cell vectors and the atomic coordinates, where x , y , and z refer to the cube axes. The atomic positions are then relaxed and the distortion energy ΔE found. The stress-energy tensor is then deduced from solving the equation $\Delta E = \text{Tr } B \cdot \epsilon$. Although only three B_{ij} are independent, the fourth element provides a check for the traceless condition. The principal directions and magnitudes of the tensor are found by diagonalization. The calculation of the tensor has already been described for interstitial and substitutional oxygen defects in Si, and a comparison with observed values shows that the errors in the principal values of the tensor are around 15%.⁴⁰

The donor and acceptor levels of a defect were calculated from the difference in total energies of charged and neutral defects, $E(0/+) = E(0) - E(+)$ and $E(-/0) = E(-) - E(0)$, respectively. However, the energy of a supercell composed of charged defects is divergent and even for a neutral cell is conditionally convergent. In practice, a compensating homogeneous background charge is added to the supercell which removes terms in the total energy arising from the long-ranged contributions due to the net charge, dipole, or quadrupole moment.⁴⁵ Thus only the difference in $E(0/+)$ between two such defects is physically relevant. We therefore calculate the donor level of a defect, denoted by $(0/+)$, by comparing $E(0/+)$ with the same quantity found for a standard defect evaluated in the same supercell. The acceptor level, denoted by $(-/0)$, is found by comparing $E(-/0)$ for the defect with a standard one. For the standard defect we take the carbon interstitial which has known donor and acceptor levels at $E_v + 0.28$ and $E_c - 0.10$ eV.⁴⁶ Clearly the method will be more accurate if systematic errors have been eliminated and this occurs if the wave functions of the defect and standard have the same symmetry and range. This implies that the defect and standard should have similar levels and treated in the same-sized cell and basis. This method

is similar to that used in the cluster method to predict donor and acceptor levels.⁴⁷ It has proved very useful in anticipating the single and second acceptor levels of Sn-V defects in Si.⁴⁸ Table II shows that the calculated $E(0/+)$ energy for C_iO_i is 6.750 eV and lies 0.084 eV above that for C_i . Since the donor level of C_i lies at $E_v + 0.28$ eV, this places the donor level of C_iO_i at $E_v + 0.364$ eV in excellent agreement with the experimental value of $E_v + 0.38$ eV.

Convergence tests were carried out with respect to the number of sampling \mathbf{k} points, the real-space basis functions, and the energy cutoff for the plane-wave expansion of the charge density.⁴⁰ Table II shows the effect of additional bond center basis functions on the formation energy of O_i , C_i , C_iO_i , C_iO_iH , and $C_iO_{2i}H$ neutral defects. The formation energy of a neutral defect is defined in terms of the chemical potentials μ_i of its constituents by

$$E_f = E(0) - \sum_i N_i \mu_i,$$

where $E(0)$ is the energy of the neutral defect in a unit cell containing N_i atoms of species i . Table II demonstrates that the E_f , $E(0/+)$, and $E(-/0)$ have converged to within ~ 0.1 eV. Thus the donor level of C_iO_i found with the larger basis now lies at $E_v + 0.408$ eV or an increase of only 0.04 eV over our previous estimate. Thus the estimates of the donor and acceptor levels have converged to about 0.1 eV.

V. THEORETICAL RESULTS

A. C_iO_i complex

In agreement with previous calculations,⁹ we find that the ground-state structure of C_iO_i is one where both carbon and oxygen are threefold coordinated and form two vertices of a ring as shown in Fig. 1(b). The structure where the O atom lies at the center of the dilated Si-Si bond, shown in Fig. 1(a), relaxes spontaneously to the ring defect for both the neutral and positively charged centers. The binding energy between C_i and O_i is 1.7 eV and this large value is consistent with the high thermal stability of the defect.

Table II shows that $E(0) - E(+)$ for C_iO_i lies 0.08 eV above that for C_i . Therefore a deep donor level lies at E_v

+0.36 eV in agreement with the observed DLTS level at $E_V+0.38$ eV.⁸ No acceptor or second donor levels were found. A Mulliken bond population analysis gives 25.4% and 0.1% of spin density localized around the carbon and oxygen atoms, respectively. The first is in agreement with the 28.6% spin localization on carbon measured for G15.² In addition, the four Si atoms bonded to Si₁ and Si₂ in Fig. 1(b) share about 15% of the unpaired spin density. The presence of oxygen rotates the Si₂-C bond through 22° away from the [010] axis. This is in excellent agreement with the angle of $\theta_A=20^\circ\pm 5^\circ$ that two of the principal directions of the ¹³C-hyperfine tensor make with the crystallographic axes.²

The principal directions of the calculated stress-energy tensor are shown in Fig. 1(b). The C_{1h} symmetry of the defect implies that one principal direction (corresponding to the B_2 component) lies along $[10\bar{1}]$ but the other directions are rotated from the [010] and the [101] axes. For the positively charged defect, the rotation angle is calculated to be $\theta_B=22^\circ$, and the principal values of the tensor are 8.5, 2.3, and -11.8 eV for B_1 , B_2 , and B_3 , respectively. The angle arises from the perturbation to the structure caused by the oxygen atom as it vanishes for the C_i defect. Stress alignment experiments give the measured values of B_1 , B_2 , and B_3 for G15 to be 8.6, 0.2, and -8.8 eV and $\theta_B=15^\circ$, and thus the model accounts well the observations.

The LVM's for the neutral and charged defects are shown in Table I. Of special interest are the oxygen-related modes. The highest of these lies at 760 cm⁻¹—well below the asymmetric stretch mode for interstitial oxygen at 1136 cm⁻¹. This is a characteristic of the weakened bonds of overcoordinated oxygen relative to those in Si-O-Si. The oxygen mode is very close to the observed band at 742.8 cm⁻¹. The observed and calculated ¹⁸O shifts are also very close, lying at 33.4 and 35.6 cm⁻¹, respectively. Two carbon-related modes are calculated to lie at 1138 and 876 cm⁻¹, close to the observed 1116 and 865 cm⁻¹ bands. Their shift with ¹³C demonstrates that they are carbon related in agreement with the observations.

The four remaining low-frequency modes at 593, 556, 545, and 544 cm⁻¹ have not been assigned previously. They arise from vibrations of Si neighbors to the defect core and are properly described only when energy second derivatives with these atoms are calculated directly from the *ab initio* program. In this sense they are similar to the lattice-induced band at 517 cm⁻¹ due to interstitial oxygen.⁴⁰ These modes display very small isotopic shifts upon C or O substitution. Frequencies and isotopic shifts of the 544 and 545 cm⁻¹ modes agree well with those of the measured 529 and 540 cm⁻¹ bands, supporting the assignment of the latter to C_iO_i (see Sec. III). However, the symmetry of the 556 and 544 cm⁻¹ modes is B and in conflict with the claim that only A modes are detected as phonon replicas. According to group theory, this is not actually the case for a C_{1h} defect, although then the dipole matrix element must involve components parallel and perpendicular to the mirror plane (or vice versa) for the zero phonon line and replica, respectively.

In summary, the agreement between the calculated and observed modes, their isotopic shifts, the energy level, and stress tensor give convincing evidence for the ring structure of C_iO_i .

TABLE III. Relative energies (eV) for five C_iO_iH structures differing in the attachment of hydrogen. R (ring) and O (open) core structures were considered. X-H represent structures where the H atom is bonded to X, where X can be C, Si₁, Si₂, or the O atom in Fig. 4. NS stands for not stable.

Core charge state	R			O		
	+	0	-	+	0	-
C-H	0.00	0.00	NS	NS	0.17	0.00
Si ₁ -H	NS	NS	NS	NS	NS	NS
Si ₂ -H	NS	NS	NS	1.67	0.89	0.53
O-H	2.93	2.89	2.32	NS	NS	NS

B. Interaction between C_iO_i and hydrogen

It is well established that hydrogen interacts effectively with both deep and shallow centers, displacing or eliminating their energy levels in the gap. Moreover, dangling bonds are particularly attractive sites for H attack.⁴⁹⁻⁵¹

The C_iO_i defect, in the neutral- or positive-charge states, possesses one fully or partially occupied p -like dangling orbital centered on the carbon atom. This is a likely place for H attachment as the carbon atom is then saturated leaving the electrical activity confined to the Si₂ dangling bond. If this is empty, as in the positively charge defect, then a ring structure involving oxygen is likely to form in the same way as in C_iO_i . However, in the neutral or negative center, an antibonding orbital will be occupied and we expect that the ring will break. This would leave an occupied dangling bond orbital on the Si radical near an oxygen atom in its normal interstitial bond-centered configuration. We call the ring structure the R form and the open configuration the O form. However, there are several other possible sites for H attachment. It could bond with silicon atoms Si₁ and Si₂ in Fig. 1(b) or with the oxygen atom. The relative energies when H is in all these structures are given in Table III for the positive-, neutral-, and negative-charge states. Our conclusion is that H prefers to bond with carbon in all cases. However, as expected, the structure depends on the charge state with the R form lowest in energy for the positive and neutral defects and the O form in the negative center.

In Fig. 4, a configuration diagram is shown for the defect. Here, quoted values correspond to the results of the calculations, and the parabolic shapes are only schematic. In the neutral defect, the R form has the lowest energy while the O form is metastable by 0.17 eV. By carefully mapping the energy surface linking the two structures, we find ~ 0.10 and ~ 0.27 eV barriers for O \rightarrow R and R \rightarrow O paths, respectively. In the positive-charge state, the ring form is again stable but the O form is now unstable and relaxes spontaneously to R.

In the negative-charge state, however, the Si₂ dangling bond is occupied with two electrons and a dative bond with oxygen cannot occur. Thus the ring form is unstable and spontaneously relaxes to the O form. Consequently the defect is bistable, taking the O form in the negative state and the R form in the positive case.

The dissociation energy of the R form into C_iH and O_i defects was estimated to be 1.4 eV. Once this dissociation has occurred, it is expected that the defects would be lost as

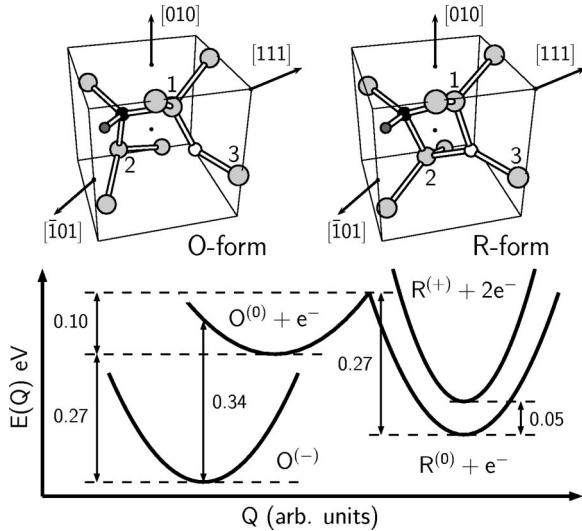


FIG. 4. Configuration coordinate diagram for C_iO_iH . Atomic structures for O and R forms are also shown. Gray, black, and white atoms are Si, C, and O, respectively. The small gray atom bonded to carbon is H. Quoted values were calculated by the total energy method.

previous theory has indicated that C_iH diffuses faster than C_i .⁵² The dissociation path involving the release of H is unlikely to occur. This is because the binding energies of H with the C_iO_i center are found to be about 2.5 eV. These were calculated by moving $H^{(-)}$ or $H^{(0)/(+)}$ from the defect and placing it at an interstitial T or BC sites, respectively.

We now consider the energy levels of the defect. These were calculated for the R and O forms separately, as these are the ground states for the positive- and negative-charge states, respectively (see Table II). The difference in energies of $O^{(-)}$ and $O^{(0)}$ when compared with $C_i^{(-)}$ and $C_i^{(0)}$ (see Sec. III) shows that the $(-/0)$ level lies at $E_c - 0.27$ eV. This is not the thermodynamic level as the neutral O form is metastable with respect to the R form. Nevertheless, it can be compared with the 0.15 eV emission barrier measured for D1 in the D form (see Fig. 2). In the R form, the $(0/+)$ level lies at $E_c - 0.05$ eV. This demonstrates that the defect is a shallow donor in one form and a deep acceptor in the other. Using the 0.17 eV difference in energies of the two neutral forms yields the thermodynamic $(-/0)$ level at $E_c - 0.1$ eV, in excellent agreement with the $(-/0)$ level at $E_c - 0.11$ eV for the D1 center described in the Introduction.

These results are summarized in Fig. 4. If the charge state of $O^{(-)}$ configuration is changed to become neutral, the energy drops 0.06 eV upon relaxation. The barrier for $R^{(0)} \rightarrow O^{(0)}$ is about 0.27 eV while $R^{(0)}$ is 0.17 eV more stable than $O^{(0)}$. The inverted order of energy levels implies that $U = E(-/0) - E(0/+) = -0.05$ eV is negative.

The bistability properties and electronic levels for C_iO_iH shown in Fig. 4 and those for the D1 defect shown in Fig. 2 are strikingly similar. Thus we identify the R and O forms with the experimentally labeled H and D forms, respectively. The experimental $(-/0)$, $(0/+)$ levels and $H^{(0)} \rightarrow D^{(0)}$ barrier energies are 0.11, 0.0426, and 0.15 eV, respectively.

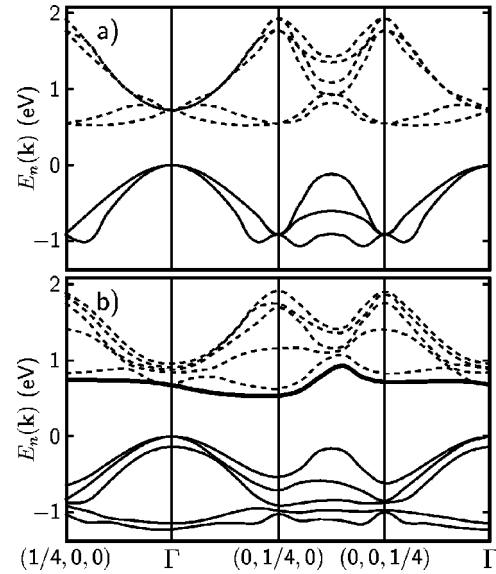


FIG. 5. One-electron band structure for bulk Si (a) and the R form of the neutral C_iO_iH defect (b) folded in 64-Si atom supercells. All \mathbf{k} vectors are in $2\pi/a_0$ units, where $a_0 = 5.390$ Å is the calculated Si lattice parameter. Alignment of the defect is as shown in Fig. 4. Solid and dashed lines represent occupied and empty bands, where the highest half-filled band is emphasized as a thick branch in (b).

The C_iO_iH complex has two paramagnetic states, with the $R^{(0)}$ form more stable, and therefore, we investigated the character of the spin density by analyzing the Mulliken populations of the highest-occupied band of the neutral defects.

In the R form, the Mulliken bond populations show only $\sim 0.5\%$ and $\sim 0.1\%$ of the spin density lying on C and H, and none on the oxygen atom. The vanishing spin density on oxygen is striking and unexpected as the overcoordinated oxygen atom is the source of donor activity. We interpret this result in the following way. The anisotropic defect creates a compressive stress along the C-Si₂ bond which is rotated by 22° away from $[010]$. This stress will split the six conduction band valleys along cube directions, lowering the energy of the pair along $[010]$ (the alignment of C-Si₂ in Fig. 4) relative to the other two pairs.⁵³ Figure 5 shows the band structure for the Si crystal folded into the 64-atom cell. The conduction band minima for Si lie near the folded X points at $\pm(2\pi/a_0)\langle\frac{1}{4}00\rangle$. However, in the case when the defect occupies the unit cell, Fig. 5 shows that the band close to the conduction-band minima near $\pm(2\pi/a_0)(0\frac{1}{4}0)$ is now pushed downward into the gap which we suggest is due to the compressive stress of the defect along (010) . This strain leads to an effective-mass gap level localized on Si atoms and this explains why the resulting state has so little amplitude on C, H, and O. In essence, the potential giving rise to the gap state is due to stress and not the chemical identity of the atoms making up the defect.

The partial occupation of the strain-induced gap level is, however, dependent on the presence of these impurities. The C atom is fully saturated and cannot lead to any donor activ-

TABLE IV. Local vibrational modes and their downward isotopic shifts (cm^{-1}) for the R and O forms of $\text{C}_i\text{O}_i\text{H}$, $\text{C}_i\text{O}_i\text{H}_2$, and $\text{C}_i\text{O}_{2i}\text{H}$ defects in the neutral charge state. For $\text{C}_i\text{O}_i\text{H}$ and $\text{C}_i\text{O}_{2i}\text{H}$, the first, second, and third rows correspond to modes which are mainly localized on C-H, C, and O atoms, respectively. For $\text{C}_i\text{O}_i\text{H}_2$, the second row gives modes localized on the Si-H unit, and the third and fourth rows list O- and C-related modes. The last four frequencies in all defects correspond to modes mainly localized on Si atoms. Starred values list the actual frequencies of modes of mixed character and not their isotopic shift.

Defect	^{12}C , ^{16}O , H	^{12}C , ^{18}O , H	^{13}C , ^{16}O , H	^{12}C , ^{16}O , D
$\text{C}_i\text{O}_i\text{H}$ R form	2754.4, 1072.3, 943.0	0.0, 0.3, 0.2	7.6, 8.7, 4.2	735.9, 978.5*, 782.3*
	933.3, 752.7	1.3, 5.1	22.1, 11.2	740.9*, 656.0*
	719.6	28.6	7.6	-1.6
	594.3, 563.3, 544.6, 530.5	1.7, 4.5, 0.2, 1.5	2.9, 0.6, 0.2, 1.0	3.9, 0.9, 6.4, 3.0
$\text{C}_i\text{O}_i\text{H}$ O form	2767.9, 1027.4, 947.9	0.0, 2.1, 0.1	7.8, 7.1, 3.9	739.9, 924.5*, 815.4*
	881.4, 790.1	0.3, 0.1	21.0, 20.1	704.8*, 665.2*
	1009.7	42.7	0.9	-3.1
	639.7, 586.9, 549.1, 531.8	6.4, 0.1, 0.0, 0.1	0.2, 4.6, 0.2, 0.4	0.1, 4.7, 4.7, 3.2
$\text{C}_i\text{O}_i\text{H}_2$	2723.4, 1032.4, 964.1	0.0, 1.1, 0.0	7.6, 9.0, 5.1	727.7, 927.1*, 839.6*
	1982.3, 772.5, 719.3	0.0, 0.0, 0.0	0.1, 6.0, 0.1	561.3, 701.8*, 672.1*
	997.9	43.3	0.2	-2.5
	878.9, 817.4	0.3, 0.1	18.3, 16.0	634.7*, 586.3*
	635.1, 588.0, 560.2, 534.0	6.5, 0.1, 0.0, 0.1	0.2, 3.7, 0.8, 0.3	0.1, 1.5, 7.5, 3.6
$\text{C}_i\text{O}_{2i}\text{H}$	2730.5, 954.6, 943.6	0.0, 2.5, 0.9	7.6, 10.5, 13.7	729.7, 999.5*, 792.1*
	1079.9, 756.9	0.5, 1.9	10.4, 17.3	737.7*, 673.0*
	1004.1, 811.3	44.6, 33.3	0.1, 2.5	-0.1, -3.4
	670.1, 569.5	12.1, 11.6	0.5, 1.4	2.1, 1.0
	593.0, 549.0	1.6, 5.8	3.4, 0.1	4.0, 0.4

ity. Consider now the trivalent oxygen atom. One of the electrons in the lone pair on oxygen forms a bond with the Si_2 radical, leaving a single electron in an antibonding level. If this level lies *above* the gap state arising from the compressive stress of the defect, then the donor electron would drop into the stress induced defect level and lose its oxygen parentage. In this way, the lack of spin density on oxygen is explained. The explanation is similar to the origin and behavior of the double-donor activity of the NL8 TDD(N) defect.⁵⁴

In the neutral O form, 30% of the spin density lies on the Si_2 radical. The wave function is composed of 15% s and 85% p (approximately parallel to $[101]$), respectively. Smaller spin densities of about 3%–4% lie on both Si atoms bound to Si_2 on the left-hand side of Fig. 4. Again, little spin density is found on carbon or oxygen. Finally, we note that in both forms the C-H bond is aligned along $\langle 110 \rangle$ —the same direction as the H-hyperfine interaction in D1.

We now turn to the local vibrational modes of the R and O forms given in Table IV. The first three rows give the modes localized mainly on C-H, C, and O, respectively. One of the most noticeable features is that the oxygen-related mode is very sensitive to its bonding. In the ring structure (R form) its LVM lies around 720 cm^{-1} but this increases to

1010 cm^{-1} for the O form where it assumes its normal bond-centered location. The C-H stretch mode lies around 2700 cm^{-1} while two wag modes are found around 1000 cm^{-1} and are split by about $80\text{--}100 \text{ cm}^{-1}$. Two carbon-related modes lie around 800 and 900 cm^{-1} , although these differ in the two forms, and four other less localized modes lie close to the Raman edge.

Calculations of ^{18}O - and ^{13}C -related isotopic shifts are shown in the second and third columns of numerical data. The oxygen-related mode has shifts of 29 and 43 cm^{-1} in the R and O forms. In the deuterated case, a complicated reordering occurs, with a change in character in some of the modes. For this reason it has not been possible to give its downward isotopic shifts and Table IV reports the calculated mode with starred values.

Of great significance is the 1009.7-cm^{-1} oxygen-related mode in the O form which shifts 3.1 cm^{-1} *upwards* with deuterium. This is close to a mode observed for the D form of D1, described in the Introduction, at 1025.5 cm^{-1} which also shifts 2.4 cm^{-1} upward with deuterium. We can now understand this anomalous shift as arising from a coupling with the undetected C-H wag mode at 1027.4 cm^{-1} . In the deuterated defect, this wag mode shifts down to around 900

cm^{-1} and below the oxygen-related mode and hence the attempted crossing leads to an increase in the frequency of the oxygen-related mode. Oxygen-related modes usually possess large effective charges while the wag and stretch modes due to C-H have not been detected presumably because of the low values of their effective charges.

In summary, the $\text{C}_i\text{O}_i\text{H}$ defect is bistable with donor and acceptor levels close to the shallow thermal donor D1 defect. The thermal stability, negative- U character, and vibrational modes are consistent with an assignment to this defect which is also known to contain H.

C. $\text{C}_i\text{O}_i\text{H}_2$ defect

The interaction between the $\text{C}_i\text{O}_i\text{H}$ defect and a second H atom was also investigated. One would then expect that the two H atoms would passivate the Si and C radicals, leading to an inert defect. Indeed, among several alternative structures, the lowest energy one is where the second hydrogen atom binds to the Si_2 radical in Fig. 4 (O form) on the opposite side of the oxygen atom. The alternative, where H binds to Si_2 nearby the oxygen, is 0.6 eV higher in energy. There are then no donor or acceptor levels and the defect is fully passivated. The oxygen atom is bound to C_iH_2 with an energy of 1.4 eV, while the second H atom is bound with an energy of ~ 2.5 eV.

Table IV gives the LVM's for the defect. These are similar to the O form of $\text{C}_i\text{O}_i\text{H}$, but there are three additional Si-H-related stretch and bend modes at 1982, 773, and 719 cm^{-1} . The O mode is now close to 1000 cm^{-1} , reflecting its divalent character. The lower carbon mode at 817 cm^{-1} is pushed up by coupling with the Si-H wag modes. As for the singly hydrogenated complex, deuteration results in a cross over and mixing of several modes. The C-H mode at 1032 cm^{-1} falls below the oxygen mode which is consequently displaced upwards from 998 to 1000 cm^{-1} in a similar manner to the $\text{C}_i\text{O}_i\text{H}$ defect.

D. $\text{C}_i\text{O}_2\text{H}$ defect

We briefly describe the effect of adding a second oxygen atom to $\text{C}_i\text{O}_i\text{H}$. There are now a greater number of candidate structures, but among those investigated, the ones with the additional O atom lying in the same $(\bar{1}01)$ plane as C_iO_i are energetically favorable. Several ring (R) and open (O) structures have low formation energies and are shown in Fig. 6. The O' structure was proposed previously as a candidate for a H-related shallow thermal donor.^{17,18}

The energies of all these forms are listed in Table V. Defects in the positive-, neutral-, and negative-charge states were considered. Once again, the R form is found to be the ground-state configuration for the neutral- and positive-charged states, whereas the O form is stable in the negative-charge state. Forms R' and O' are metastable by ~ 0.5 eV, with a slight preference for the asymmetric R form.

The electronic levels were evaluated for the R and O forms. Again, the former is a shallow donor with a calculated level at $E_c - 0.01$ eV. The O form has a deep $(-/0)$ level at $E_c - 0.3$ eV, and the barrier for the $\text{O}^{(0)} \rightarrow \text{R}^{(0)}$ transition is

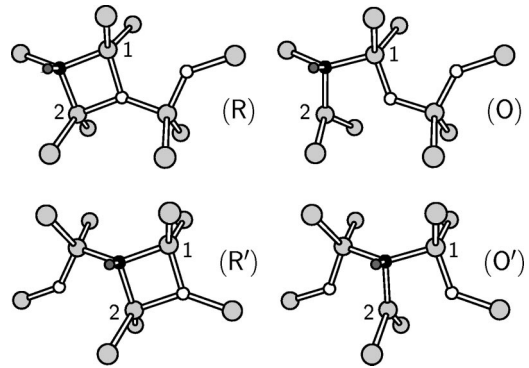


FIG. 6. Structures for $\text{C}_i\text{O}_2\text{H}$ considered in our study. Gray, black, and white atoms are Si, C, and O. The small gray atom is H. Relative energies are listed in Table V.

only 0.02 eV. However, the $\text{O}^{(0)}$ form is now metastable by 0.56 eV compared with 0.17 eV for $\text{C}_i\text{O}_i\text{H}$. This shows that the thermodynamic $(-/0)$ level is now above the conduction-band bottom and hence the defect can never be prepared in the negative-charge state. These results are summarized in Fig. 7. Thus $\text{C}_i\text{O}_2\text{H}$ is *not* bistable.

Our conclusions are then that the ring form is stabilized in $\text{C}_i\text{O}_2\text{H}$ which can only be a shallow donor defect. This is consistent with an assignment to D2, and therefore to STD(H)2, as this defect is not known to be bistable.

The LVM's of the $\text{R}^{(0)}$ are given in Table IV. The C-H stretch mode lies around 2700 cm^{-1} , well above a series of strongly coupled C-H modes. Two O modes appear at 1004 and 811 cm^{-1} , consistent with the presence of a divalent and trivalent oxygen. Modes around 600 cm^{-1} also shift considerably with ^{18}O substitution. These are similar to a low-frequency pair also found in the interstitial oxygen dimer.^{40,55,56}

VI. CONCLUSIONS

Absorption bands produced by the $\text{C}_i\text{O}_i^{(0)}$ defect have been studied in detail. FTIR data were obtained from Si

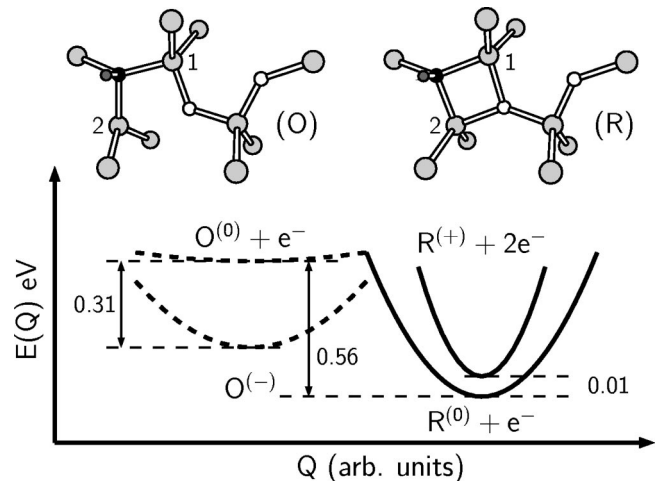


FIG. 7. Configurational diagram for the $\text{C}_i\text{O}_2\text{H}$ defect. Dashed potential curves indicate that the O form is unstable under thermodynamic equilibrium—the $\text{C}_i\text{O}_2\text{H}$ complex is a single shallow donor.

TABLE V. Relative energies (eV) for four C_iO_2H structures R, O, R', and O' shown in Fig. 6. NS stands for not stable.

Charge state	+	0	-
R	0.00	0.00	NS
O	NS	0.56	0.00
R'	0.37	0.45	NS
O'	0.61	0.56	NS

samples doped with three combinations of dominant oxygen and carbon isotopes, including the effect of ^{18}O . We found that the IR activity from the C_iO_i defect can be divided into three sets of bands classified according to their isotopic shifts. The carbon-related 1116 and 865 cm^{-1} bands, the oxygen 742 cm^{-1} band, and the four low-frequency 585, 550, 540, and 529 cm^{-1} bands, where the 585 and 540 cm^{-1} bands, have not been reported previously. Of particular interest is the position and ^{18}O isotopic shift observed for the 742 cm^{-1} band (33.4 cm^{-1}), much less pronounced than that of O_i (51.4 cm^{-1}).³⁹ There is evidence for absorption bands with similar character related to the thermal double donors in Si. These lie at ~ 720 cm^{-1} and shift by ~ 24 cm^{-1} in ^{18}O -rich samples.^{57,58} These observations favor here a different bonding of oxygen, as an alternative to the *normal* bond-centered location.

The calculations have shown that the C_iO_i defect has a ring structure involving an overcoordinated oxygen atom. The weak oxygen bonding then leads to the highest oxygen-related vibrational band lying around 720 cm^{-1} and far from the 1136 cm^{-1} band of interstitial oxygen. This supports previous studies of the defect.^{9,10} This mode is relatively unaffected when H is added to the defect and appears to be a signature for this type of oxygen. All seven observed band frequencies and their isotopic shifts are remarkably well described by the model. The calculated donor level and energy-stress tensor are also in good agreement with the measured values.

The defect can trap one or two H atoms and is electrically inert in the latter. The single hydrogenated center has remarkable properties. It is bistable—i.e., the negative-charge

state has a divalent oxygen atom—whereas in the positively charged defect the oxygen is overcoordinated. The effective ionization correlation term U is negative and a shallow donor level lies 0.05 eV above a deep acceptor.

None of the calculated levels are in agreement with an assignment to the hole trap H4 at $E_v+0.28$.¹² On the other hand, the C_iO_iH defect has similar properties to the first species of a family of shallow donors, labeled DN, found in irradiated Si.^{14,21–25} D2 and D3 have been associated with the shallow thermal donor defects STD(H)2 and STD(H)3.^{16,21} The energy levels, the oxygen related vibrational mode, and its shift with hydrogen are all consistent with an assignment of C_iO_iH and $C_iO_{2i}H$ with D1 and D2, respectively. The negligible spin densities on C, H, and O and the alignment of the C-H bond along $[101]$ are consistent with ENDOR results. However, to our knowledge, no DN defects have been detected in H plasma or wet chemical etched and irradiated Cz-Si samples. Moreover, the presence of carbon and oxygen in the defects remains to be verified by a spectroscopic technique. According to the calculations, the ground state for the effective-mass $R^{(0)}$ defect is localized on a strain-induced gap level mainly localized on Si atoms. The donor character originates from the overcoordinated oxygen atom which possesses a level higher up in energy. The electron in this level then falls into the strain-induced gap level. Thus the character of the spin density of the donor level does not reflect its oxygen parentage and this is consistent with the ENDOR studies. Thus, as for the NL8 thermal double-donor defects, the chemical composition of the DN and STD(H)N families may be difficult to determine by magnetic resonance.

Finally, we point out that other STD models could be obtained by substituting the C_i -H unit in $C_iO_{n_i}H$ defects by a group-III atom or indeed, a complex with equivalent coordination. In particular, Al and N are obvious candidates for the STD(Al) and STD(X) families.²⁰

ACKNOWLEDGMENTS

We thank EPSRC in the UK and TFR in Sweden for financial support. We also acknowledge support from INTAS under Grant No. 97-0824.

¹G.D. Watkins and K.L. Brower, Phys. Rev. Lett. **36**, 1329 (1976).

²J.M. Trombetta and G.D. Watkins, Appl. Phys. Lett. **51**, 1103 (1987).

³J.M. Trombetta and G.D. Watkins, in *Defects in Electronic Materials*, edited by M. Stavola, S. J. Pearton, and G. Davies, Mater. Res. Soc. Symp. Proc. No. 104 (Materials Research Society, Pittsburgh 1988), p. 93.

⁴A.V. Yuhnevich, V.D. Tkachev, and M.V. Bortnik, Sov. Phys. Solid State **8**, 1044 (1966).

⁵W. Kurner, R. Sauer, A. Dörnen, and K. Tonke, Phys. Rev. B **39**, 13 327 (1989).

⁶E.C. Lightowlers and A.N. Safonov, Mater. Sci. Forum **258-263**, 617 (1997).

⁷G. Davies A.S. Oates, R.C. Newman, R. Wooley, E.C. Lightowlers, M.J. Binns, and J.G. Wilkes, J. Phys. C **19**, 841 (1986).

⁸P.M. Mooney, L.J. Cheng, M. Suli, J.D. Gerson, and J.W. Corbett, Phys. Rev. B **15**, 3836 (1977).

⁹R. Jones and S. Öberg, Phys. Rev. Lett. **68**, 86 (1992).

¹⁰L.C. Snyder, R. Wu, and P. Deák, in Ref. 11, p. 419.

¹¹*Early Stages of Oxygen Precipitation in Silicon*, Vol. 17 of NATO Advanced Study Institute, Series B: Physics, edited by R. Jones (Kluwer Academic, Dordrecht, 1996).

¹²O.V. Feklisova and N.A. Yarykin, Semicond. Sci. Technol. **12**, 742 (1997).

¹³O. Feklisova, N. Yarykin, Eu. Yakimov, and J. Weber, in *Proceedings of the 21st International Conference on Defects in Semiconductors*, Giessen, 2001 [Physica B (to be published)].

¹⁴V.P. Markevich, M. Suezawa, K. Sumino, and L.I. Murin J. Appl. Phys. **76**, 7347 (1994).

¹⁵R.C. Newman, J.H. Tucker, N.G. Semaltianos, E.C. Lightowlers,

- T. Gregorkiewicz, I.S. Zevenbergen, and C.A.J. Ammerlaan, *Phys. Rev. B* **54**, R6803 (1996).
- ¹⁶R.C. Newman, M.J. Ashwin, R.E. Pritchard, and J.H. Tucker, *Phys. Status Solidi B* **210**, 519 (1998).
- ¹⁷C.P. Ewels, R. Jones, S. Öberg, J. Miro, and P. Deák, *Phys. Rev. Lett.* **77**, 865 (1996).
- ¹⁸C.P. Ewels, R. Jones, and S. Öberg, in Ref. 11, p. 141.
- ¹⁹T. Gregorkiewicz, D.A. van Wezep, H.H.P.Th. Bekman, and C.A.J. Ammerlaan, *Phys. Rev. Lett.* **59**, 1702 (1987).
- ²⁰T. Gregorkiewicz, H.H.P.Th. Bekman, and C.A.J. Ammerlaan, *Phys. Rev. B* **38**, 3998 (1988).
- ²¹V.P. Markevich, T. Mchedlidze, M. Suezawa, and L.I. Murin, *Phys. Status Solidi B* **210**, 545 (1998).
- ²²V.P. Markevich, I.F. Medvedeva, L.I. Murin, T. Sekiguchi, M. Suezawa, and K. Sumino, *Mater. Sci. Forum* **196-201**, 945 (1995).
- ²³V.P. Markevich, L.I. Murin, T. Sekiguchi, and M. Suezawa, *Mater. Sci. Forum* **258-263**, 217 (1997).
- ²⁴V.P. Markevich, T. Mchedlidze, and M. Suezawa, *Phys. Rev. B* **56**, R12 695 (1997).
- ²⁵V.P. Markevich, M. Suesawa, and L.I. Murin, *J. Appl. Phys.* **84**, 1246 (1998).
- ²⁶J.R. Morton and K.F. Preston, *J. Mater. Res.* **30**, 577 (1977).
- ²⁷B. Langhanki, S. Greulich-Weber, J.-M. Spaeth, V.P. Markevich, L.I. Murin, T. Mchedlidze, and M. Suezawa, *Physica B* **302-303**, 212 (2001).
- ²⁸C. A. J. Ammerlaan, I. S. Zevenbergen, Yu. V. Martynov, and T. Gregorkiewicz, in Ref. 11, p. 61.
- ²⁹B.G. Svensson, A. Hallen, and B.U.R. Sundqvist, *Mater. Sci. Eng., B* **4**, 285 (1989).
- ³⁰E. Artacho and F. Ynduráin, *Solid State Commun.* **72**, 393 (1989).
- ³¹K. Bonde Nielsen, L. Dobaczewski, K. Goscinski, R. Bendesen, O. Andersen, and B. Bech Nielsen, *Physica B* **273-274**, 167 (1999).
- ³²A.R. Peaker, J.H. Evans-Freeman, P.Y.Y. Kan, L. Rubaldo, I.D. Hawkins, K.D. Vernon-Parry, and L. Dobaczewski, *Physica B* **273-274**, 243 (1999).
- ³³V.P. Markevich, L.I. Murin, M. Suesawa, J.L. Lindström, J. Coutinho, R. Jones, P.R. Briddon, and S. Öberg, *Phys. Rev. B* **61**, 12 964 (2000).
- ³⁴A.N. Safonov, E.C. Lightowers, G. Davies, P. Leary, R. Jones, and S. Öberg, *Phys. Rev. Lett.* **77**, 4812 (1996).
- ³⁵A. Baghdadi, W.M. Bullis, M.C. Croarkin, L. Yue-zhen, R.I. Scace, R.W. Series, P. Stallhofer, and M. Watanabe, *J. Electrochem. Soc.* **136**, 2015 (1989).
- ³⁶G. Davies and R.C. Newman, in *Handbook on Semiconductors*, edited by T. S. Moss (Elsevier Science, Amsterdam, 1994), Vol. 3b, p. 1557.
- ³⁷E.V. Lavrov, L. Hoffman, and B. Bech Nielsen, *Phys. Rev. B* **60**, 8081 (1999).
- ³⁸R.C. Newman and A.R. Bean, *Radiat. Eff.* **8**, 189 (1971).
- ³⁹B. Pajot, E. Artacho, C.A.J. Ammerlaan, and J.-M. Spaeth, *J. Phys.: Condens. Matter* **7**, 7077 (1995).
- ⁴⁰J. Coutinho, R. Jones, P.R. Briddon, and S. Öberg, *Phys. Rev. B* **62**, 10 824 (2000).
- ⁴¹H.J. Monkhorst and J.D. Pack, *Phys. Rev. B* **13**, 5188 (1976).
- ⁴²R. Jones and P. R. Briddon, in *Identification of Defects in Semiconductors*, edited by M. Stavola, Semiconductors and Semimetals, Vol. 51A (Academic Press, San Diego, 1998), p. 288.
- ⁴³G.D. Watkins, in Ref. 11, p. 1.
- ⁴⁴In order to obtain the traceless strain-energy tensor B , one can skip the volume relaxation step if a linear lattice-defect coupling is assumed, i.e., $B = B' - 1/3 \text{Tr } B'$, where B' is the nontraceless tensor.
- ⁴⁵L. Kleinman, *Phys. Rev. B* **24**, 7412 (1981).
- ⁴⁶L.W. Song, X.D. Zhan, B.W. Benson, and G.D. Watkins, *Phys. Rev. B* **42**, 5765 (1990).
- ⁴⁷A. Resende, R. Jones, S. Öberg, and P.R. Briddon, *Phys. Rev. Lett.* **82**, 2111 (1999).
- ⁴⁸A. Nylandstead Larsen, J.J. Goubet, P. Mejlholm, J. Sherman Christensen, M. Fanciulli, H.P. Gunnlaugsson, G. Weyer, J. Wulff Petersen, A. Resende, M. Kaukonen, R. Jones, S. Öberg, P.R. Briddon, B.G. Svensson, J.L. Lindström, and S. Dannefaer, *Phys. Rev. B* **62**, 4535 (2000).
- ⁴⁹S.J. Pearton, J.W. Corbett, and M. Stovola, *Hydrogen in Crystalline Semiconductors* (Springer-Verlag, Berlin, 1992).
- ⁵⁰R. Jones, B.J. Coomer, J.P. Goss, B. Hourahine, and A. Resende, *Solid State Phenom.* **71**, 173 (2000).
- ⁵¹E.C. Lightowers, R.C. Newman, and J.H. Tucker, *Semicond. Sci. Technol.* **9**, 1370 (1994).
- ⁵²P. Leary, R. Jones, and S. Öberg, *Phys. Rev. B* **57**, 3887 (1998).
- ⁵³A.K. Ramdas and S. Rodriguez, *Rep. Prog. Phys.* **44**, 1297 (1981).
- ⁵⁴R. Jones, J. Coutinho, S. Öberg, and P.R. Briddon, in *Proceedings of the 21st International Conference on Defects in Semiconductors*, Giessen, 2001 [Physica B (to be published)].
- ⁵⁵S. Öberg, C.P. Ewels, R. Jones, T. Hallberg, J.L. Lindström, L.I. Murin, and P.R. Briddon, *Phys. Rev. Lett.* **81**, 2930 (1998).
- ⁵⁶M. Pesola, J. von Boehm, and R.M. Nieminen, *Phys. Rev. Lett.* **82**, 4022 (1999).
- ⁵⁷J.L. Lindström and T. Hallberg, *Phys. Rev. Lett.* **72**, 2729 (1994).
- ⁵⁸J.L. Lindström and T. Hallberg, in Ref. 11, p. 41.